ISBN: 978-3-95450-248-6 ISSN: 2673-5490 doi: 10.18429/JACoW-IPAC2025-WEPM031

SIMULATION-BASED OPTIMIZATION OF THE INJECTION OF ULTRASHORT NON-GAUSSIAN ELECTRON BEAMS INTO A STORAGE RING

J. Schäfer*, M. Fuchs, B. Härer, A.-S. Müller, R. Ruprecht, M. Schuh, M. Schwarz, C. Xu†
Karlsruhe Institute of Technology, Karlsruhe, Germany

Abstract

The compact STorage ring for Accelerator Research and Technology (cSTART) project at the Karlsruhe Institute of Technology (KIT, Germany) aims to explore non-equilibrium electron beam dynamics and injection of laser-plasma accelerator (LPA) bunches. The Very Large Acceptance compact Storage Ring (VLA-cSR) is also filled by a second injector that can deliver ultrashort bunches from the Ferninfrarot Linac- Und Test-Experiment (FLUTE). Injection from FLUTE into the VLA-cSR is achieved via a complex 3D Injection Line (IL) featuring tilted deflections, negative dispersion, and extreme compression to femtosecond bunch lengths.

From this transport, the bunch develops pronounced non-Gaussian tails; nevertheless, near the injection point, it is crucial to ensure matching to both the dynamic aperture and the periodic solutions of the storage ring dynamics. The 25 quadrupole magnets of the injection line make conventional optimization methods impractical. This contribution discusses the development of magnet optics to meet these extreme requirements. The optimization task was divided into two parts: longitudinal compression was addressed using a surrogate model, while transverse matching is currently being pursued with Bayesian optimization.

INTRODUCTION

The cSTART project at the Karlsruhe Institute of Technology (KIT) aims to inject and store laser-plasma accelerator (LPA) [1] bunches in the uniquely designed Very Large Acceptance compact Storage Ring (VLA-cSR) [2, 3]. It explores non-equilibrium beam dynamics with damping times far exceeding storage times, posing challenges in beam dynamics [4, 5], lattice design [6], diagnostics [7], magnet design [8, 9], tolerances [10] and vacuum [11]. In addition to LPA injection, the VLA-cSR is filled with ultrashort bunches from FLUTE [12], a flexible test facility for advanced beam diagnostics and dynamics [13–15].

The injection line (IL) features a complex geometry with vertical, tilted, and horizontal deflections. Bridges a 3 m height gap, fits within tight spatial constraints, and delivers femtosecond-scale bunches across a wide parameter range: 40 – 90 MeV energy and 1 pC to 1 nC bunch charge.

Figure 1 shows the cSTART project with FLUTE on the ground floor, VLA-cSR on the first floor, and IL connecting them with its division into three sections:

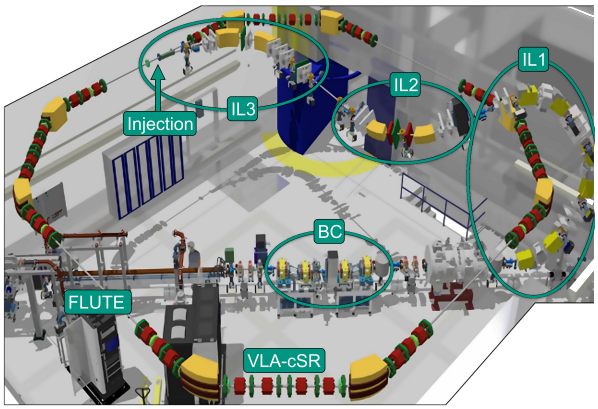

Figure 1: CAD drawing of the cSTART project, showing FLUTE, the Injection Line and the VLA-cSR storage ring.

- **IL1:** A vertical 200° arc composed of 3 DBA-like cells, lifting the beam around the storage ring.
- **IL2:** A tilted double bend achromat (DBA) section that returns the beam tube to the horizontal plane.
- **IL3:** The final matching section, which prepares the bunch for injection through the septum.

The initial IL lattice was designed for a fixed configuration [16]. As the cSTART project explores different optics (e.g., low- and negative-alpha) [17] and varying beam parameters, a flexible and robust IL optimization strategy is needed.

OPTICS STRATEGY

The IL must compress the bunch longitudinally, match the transverse phase space with the acceptance of the storage ring, and minimize beam losses. With 25 quadrupoles, 10 dipoles, and 3 sextupoles, the system provides sufficient degrees of freedom (DOF) but poses a complex optimization challenge.

To simplify this challenge, it is divided into two largely decoupled tasks: longitudinal compression and transverse matching. Quadrupoles always affect transverse optics, but influence longitudinal dynamics only when located in dispersive regions. This allows longitudinal compression to be addressed first by tuning dispersive quadrupoles, followed by transverse matching using the remaining elements.

Bunch compression is achieved when the Full Compression Condition (FCC) is fulfilled. Therefore, the sum of the

* jens.schaefer2@kit.edu
† now at Argonne National Laboratory, Lemont, IL, United States

ISBN: 978-3-95450-248-6 ISSN: 2673-5490 doi: 10.18429/JACoW-IPAC2025-WEPM031

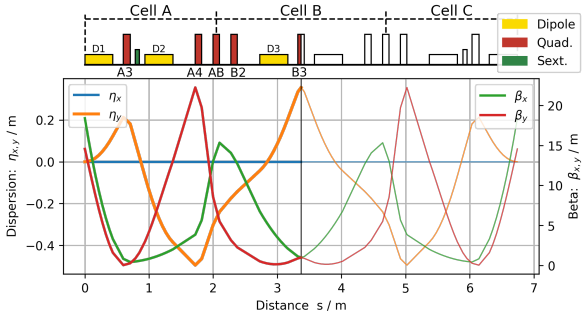

Figure 2: IL1 section with dispersion $\eta_{(x,y)}$ and $\beta_{(x,y)}$ functions. The magnetic lattice and the optics are mirror symmetric around the central quadrupole B3.

transport matrix elements R_{56} for the achromatic sections has to compensate the initial bunch momentum chirp h:

$$\sum_i R_{56,i} = -\frac{1}{h}, \quad h = \frac{\partial \delta_p}{\partial z}.$$

Although IL2 and IL3 contribute fixed or weakly tunable R_{56} values, IL1 offers sufficient flexibility to meet the FCC. In the following, we present the longitudinal optimization using a surrogate model and outline the process of transverse matching via Bayesian optimization.

LONGITUDINAL OPTICS WITH SURROGATE MODEL

The FLUTE linac can generate a variety of bunch configurations. This study uses the same chirp value as in previous studies [18]: $h = -35.5\,\mathrm{m}^{-1}$. The FLUTE bunch compressor (BC) was set to $R_{56} = -2.5\,\mathrm{cm}$, allowing for operational tuning of $\pm 2.5\,\mathrm{cm}$. IL2, a tilted DBA, contributes a fixed $R_{56} = 3.4\,\mathrm{cm}$.

IL3 includes two dipoles, the septum, kicker, and three quadrupoles in dispersion. These are used to match dispersion η and enforce $\eta'_{\mathrm{IP}} = 0$, providing two constraints with three DOF. As the third objective a minimization of the total section focusing strength was achieved using `elegant` [19], yielding $R_{56} = 20.1\,\mathrm{cm}$.

For ideal bunch compression, IL1 has to provide[1]:

$$R_{56,\mathrm{IL1}} = -\frac{1}{h} - R_{56,\mathrm{BC}} - R_{56,\mathrm{IL2}} - R_{56,\mathrm{IL3}} = -17.7\,\mathrm{cm}.$$

The FCC itself is formulated with a small tolerance:

$$\Delta R_{56}(\mathrm{IL1}) = |R_{56}(\mathrm{IL1}) + 17.7\,\mathrm{cm}| < 0.5\,\mathrm{mm}. \quad (1)$$

Figure 2 shows the IL1 lattice, composed of three DBA-like cells (A, B, C), each with two dipoles and a central quadrupole (A3, B3, C3). Three additional quadrupoles (A4, AB, B2) sit between the cells. The layout is mirror-symmetric about B3. The strong quadrupoles A3 and C3 (up to $K_1 = 80\,\mathrm{m}^{-2}$) enable negative dispersion and R_{56} values from −4.2 m to 1.3 m; all others reach up to $\pm 45\,\mathrm{m}^{-2}$.

[1] Due to rounding, the values appear not to add up exactly.

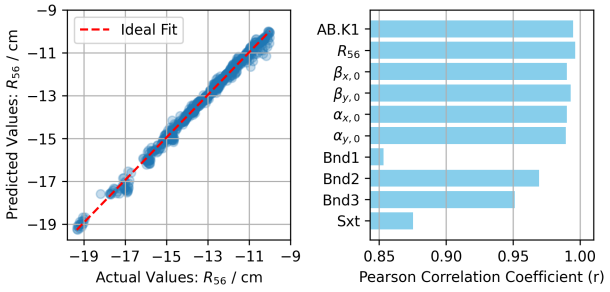

Figure 3: Neural network prediction compared to the test dataset. Left: predicted vs. simulated R_{56} values. Right: PCC for all predicted parameters.

To define a consistent symmetric optics set, the Twiss parameters at the symmetry point of IL1 are fixed:

$$\alpha_{(x,y)}(s_{\mathrm{sym}}) = 0, \quad \beta_{(x,y)}(s_{\mathrm{sym}}) = 1.$$

As a boundary condition zero dispersion at the beginning $\eta_{(x,y)}(s_0) = 0$ and mirror symmetry, the achromaticity requirement demands:

$$\eta'_{(x,y)}(s_{\mathrm{sym}}) = 0. \quad (2)$$

The IL1 section has five DOF (strengths of A3, A4, AB, B2, B3) and two objectives: FCC and achromaticity. The problem has three more degrees of freedom than constraints.

A set of optics simulations was performed using `elegant`. In each simulation, the quadrupole AB was optimized using the built-in simplex algorithm to fulfill the achromaticity condition. The remaining four quadrupole strengths (A3, A4, B2, B3) were fixed for each run. This lightweight optics simulation was repeated on a coarse 4D hypervolume, varying the K_1 values of the four quadrupoles. In total, 16,400 simulations were performed.

A neural network (NN) was trained on this data set to construct a surrogate model. Filtering the data set beforehand to include only simulations with $-20\,\mathrm{cm} < R_{56} < -10\,\mathrm{cm}$ significantly improves the performance of the model. This filtered data set contained 6,400 samples, which were split 9:1 into training and test sets. Each simulation provided the following data:

- **Input:** K_1 values of quadrupoles A3, A4, B2, B3
- **Output:**
  - Required quadrupole AB strength (K_1)
  - R_{56} of the IL1 section
  - Entrance Twiss parameters: $\alpha_{x,y}$, $\beta_{x,y}$
  - Integrated product $\int \beta_y(s) \cdot \eta_y(s)\, ds$ inside the sextupole and each of the three dipoles.

The model is a fully connected feedforward NN with 6 layers, 32 neurons, and the rectified linear unit (ReLU) activation function. It was trained using PyTorch [20], Adam optimizer, and mean squared error (MSE) loss over 1000 epochs. All data were Min-Max normalized.

The model demonstrates excellent performance. As an example, the predicted vs. simulated R_{56} is presented in

ISBN: 978-3-95450-248-6 ISSN: 2673-5490 doi: 10.18429/JACoW-IPAC2025-WEPM031

Fig. 3 (left). The prediction quality is indicated by the Pearson correlation coefficients for each parameter, where the NN scored approximately 0.99 for 6 of the 10 parameters (right). The $\beta_y \cdot \eta_y$ integrals showed a lower correlation and were excluded from further use.

The trained NN can be used to search for optimized optics configurations, for example via genetic algorithms. However, initially it was used to generate a finely gridded surrogate dataset, similar to the approach in [21]. The surrogate model was then used to explore the relationships between input and output parameters and to gain deeper insights into the underlying dynamics.

An example is shown in Fig. 4, where the surrogate model was filtered using the FCC (Eq. (1)) and an additional constraint $\beta_{x,y} < 20\,\mathrm{m}$ to exclude impractical optics. The figure shows two 2D histograms of quadrupole strengths satisfying these conditions. A strong linear dependence of A3 and B3 is visible, confirming their dominant role in driving the dispersion negative. In contrast, A4 and B2 show a more complex correlation, although a "dead zone" appears in the upper left corner of the parameter space. Note that the color scale in the histogram reflects the number of valid combinations found for each bin, not a beam optics parameter itself. The blue dots indicate the original coarse simulation grid, which highlights how the surrogate model enriches the parameter space despite the limited number of simulations.

Based on insights gained from the surrogate model, the optimization criteria for IL1 were formulated to $\beta_{x,y} < 20\,\mathrm{m}$ and a minimization of $\alpha_{x,y}$. With these criteria, an optimized configuration of K1 values was identified:

A3 = -72, A4 = -25, AB = 20, B2 = 5, B3 = -47 $[\mathrm{m}^{-2}]$.

This solution was validated in simulation and corresponds to the optics shown in Fig. 2.

TRANSVERSE OPTICS WITH BAYESIAN OPTIMIZATION

With IL1 optimized and IL2 configured using conventional methods, the remaining task is to guide the beam through IL3 and match it to the storage ring acceptance. IL2 offers limited DOF, which was used to ensure rotational symmetry at the entrance of the tilted dispersive section to mitigate emittance growth.

The dispersion-free quadrupoles in IL2 and IL3 provide the remaining six DOF. Due to nonlinear effects and the non-Gaussian nature of the beam, full 6D tracking simulations are required, making the calculations computationally much more expensive compared to previously discussed optics calculations and a NN not feasible in a reasonable time. To efficiently solve this optimization problem, Bayesian Optimization (BO) was employed using the `xopt` Python package [22], with parallelized batched simulations for speed-up.

BO is ideal for this task because of its ability to converge with relatively few data points. It also allows for custom objective functions. One candidate function under investigation is:

$$f = L \cdot \sum_i m_i,$$

where L quantifies beam losses (in %) and m_i is a matching metric for each parameter ($\beta_{x,y}$, $\alpha_{x,y}$, $\eta_{x,y}$), computed from the tracked particle distribution. For computing the Twiss parameter, a 95% quantile of the tracked particle distribution was considered to reduce sensitivity to outliers and long tails in the particle distribution.

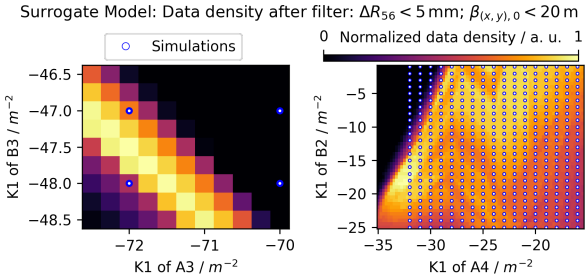

Figure 4: Density plot of optics configurations predicted by the surrogate model that satisfy FCC and $\beta_{x,y} < 20\,\mathrm{m}$ across the quadrupole strengths K1 (A3, A4, B2, B3). The blue dots indicate the original coarse simulation grid.

Each m_i is calculated using the a sensitivity function inspired by `elegant`'s `sene` (soft-edge not-equal) function:

$$\mathrm{sene}(V_1, V_2) = \frac{|V_1 - V_2|}{\tau |V_1|} \cdot H\left(|V_1 - V_2| - \tau |V_1|\right),$$

where V_1 is the target value of the VLA-cSR optics, V_2 the current value, $\tau = 0.001$ the relative tolerance, and H the Heaviside function. This formulation filters out minor deviations and emphasizes significant mismatches between the target and the actual value. This sene function thus helps guide the optimization toward well-matched solutions.

The BO of matching is currently under development, with ongoing investigations into optimal formulations of the objective function.

CONCLUSION

We present a strategy to optimize the injection line optics for transporting bunches from the FLUTE linac into the VLA-cSR storage ring. It combines a neural network surrogate model for longitudinal dynamics and femtosecond bunch compression with Bayesian optimization for transverse matching of bunches that develop non-Gaussian features during transport.

This dual-method framework enables efficient and flexible adaptation to varying beam and ring configurations, significantly improving over previous methods. The techniques discussed show strong potential for broader application in accelerator physics.

REFERENCES

[1] N. Ray *et al.*, "Laser-plasma injector for an electron storage ring", in *Proc. IPAC'24*, Nashville, TN, USA, May 2024, pp. 557–560. doi:10.18429/JACoW-IPAC2024-MOPR44

ISBN: 978-3-95450-248-6 ISSN: 2673-5490 doi: 10.18429/JACoW-IPAC2025-WEPM031

[2] M. Schwarz *et al.*, "Recent Developments of the cSTART Project", in *Proc. FLS'23*, Lucern, Switzerland, Aug. 27–Sep. 1, 2023, pp. 155–158. doi:10.18429/JACoW-FLS2023-TU4P34

[3] B. Härer *et al.*, "Non-Linear Features of the cSTART Project", in *Proc. IPAC'19*, Melbourne, Australia, May 2019, pp. 1437–1440. doi:10.18429/JACoW-IPAC2019-TUPGW020

[4] M. Schwarz *et al.*, "Impact of the cSTART impedance on beam dynamics", presented at IPAC'25, Taipei, Taiwan, Jun. 2025, paper WEPM080, this conference.

[5] M. Schwarz *et al.*, "Longitudinal beam dynamics for different initial distributions at cSTART", in *Proc. IPAC'23*, Venice, Italy, May 2023. doi:10.18429/JACoW-IPAC2023-WEPL167

[6] A. Papash *et al.*, "Beamline to inject laser plasma accelerated electrons to a quasi-isochronous compact storage ring", presented at IPAC'25, Taipei, Taiwan, June 2025, paper TUPS003, this conference.

[7] D. El Khechen *et al.*, "Characterisation of the foreseen turn-by-turn beam position instrumentation for the cSTART storage ring", presented at IPAC'25, Taipei, Taiwan, June 2025, paper THPS094, this conference.

[8] A. Bernhard *et al.*, "Magnetic design of the cSTART magnets", presented at IPAC'25, Taipei, Taiwan, June 2025, paper WEPB026, this conference.

[9] A. Bernhard *et al.*, "Compact quadrupole-sextupole magnet units for the FLUTE-cSTART injection line", presented at IPAC'25, Taipei, Taiwan, June 2025, paper WEPB027, this conference.

[10] P. Schreiber *et al.*, "Alignment tolerance studies for the cSTART storage ring", presented at IPAC'25, Taipei, Taiwan, June 2025, paper WEPM038, this conference.

[11] B. Krasch *et al.*, "Conceptual design of the vacuum system of cSTART", presented at IPAC'25, Taipei, Taiwan, June 2025, paper THPB001, this conference.

[12] M. J. Nasse *et al.*, "FLUTE: A versatile linac-based THz source", *Rev. Sci. Instrum.*, vol. 84, no. 2, p. 022705, Feb. 2013. doi:10.1063/1.4790431

[13] J. Schäfer, "Feasibility studies for a Transverse Deflecting Structure measurement at FLUTE", Ph.D. thesis, Karlsruher Institut für Technologie (KIT), Karlsruhe, Germany, May 2024. doi:10.5445/IR/1000170357

[14] M. Nabinger *et al.*, "Terahertz Streaking Detection for Longitudinal Bunch Diagnostics at FLUTE", presented at IPAC'25, Taipei, Taiwan, June 2025, paper THPM064, this conference.

[15] S. Glukhov *et al.*, "Possibilities for performance enhancement of a compact TDS at FLUTE", presented at IPAC'25, Taipei, Taiwan, June 2025, paper THPM087, this conference.

[16] J. Schaefer, "Lattice design of a transfer line for ultra-short bunches from FLUTE to cSTART", M.Sc. thesis, Phys. Dept., Karlsruher Institut für Technologie (KIT), Karlsruhe, Germany, 2019. doi:10.5445/IR/1000105061

[17] A. I. Papash *et al.*, "Modified Lattice of the Compact Storage Ring in the cSTART Project at Karlsruhe Institute of Technology", in *Proc. IPAC'21*, Campinas, Brazil, May 2021. doi:10.18429/JACoW-IPAC2021-MOPAB035

[18] J. Schaefer *et al.*, "Dynamic Aperture Studies for the Transfer Line From FLUTE to cSTART", in *Proc. IPAC'22*, Bangkok, Thailand, Jun. 2022, doi:10.18429/JACoW-IPAC2022-MOPOST041

[19] M. Borland, "elegant: A Flexible SDDS-Compliant Code for Accelerator Simulation", presented at ICAP'20, Rep. LS-287, Sept. 2000. doi:10.2172/761286

[20] A. Paszke *et al.*, "PyTorch: An Imperative Style, High-Performance Deep Learning Library", in *Proc. NIPS'19*, 2019, pp. 8024–8035. doi:10.5555/3454287.3455008

[21] C. Xu *et al.*, "Surrogate Modelling of the FLUTE Low-Energy Section", in *Proc. IPAC'22*, Bangkok, Thailand, Jun. 2022. doi:10.18429/JACoW-IPAC2022-TUPOPT070

[22] R. Roussel *et al.*, "Xopt: A simplified framework for optimization of accelerator problems using advanced algorithms", in *Proc. IPAC'23*, Venice, Italy, 2023. doi:10.18429/JACoW-IPAC2023-THPL164